Spherulitic morphology of isotactic polypropylene investigated by scanning electron microscopy

M. Aboulfaraj*, B. Ulrich, A. Dahoun and C. G'Sell
Laboratoire de Métallurgie Physique et Science des Matériaux, URA CNRS No. 155, Ecole des Mines, Parc de Saurupt, 54042 Nancy, France
(Received 24 July 1992; revised 28 January 1993)

The aim of this work is to investigate the complex spherulitic structure of bulk polypropylene samples from direct scanning electron microscopy (SEM) observations of etched surfaces. Thick plates of isotactic polypropylene were moulded by intrusion. Preliminary characterization, involving X-ray diffraction, microdensitometry and differential scanning calorimetry (d.s.c.), showed that the slow solidification process develops a variable proportion of the monoclinic (α) and hexagonal (β) phases, ranging from 0% of β-crystals at the surface to 60 vol% of this phase at the core. In addition, samples were cut across the thickness of the plates, finely polished and then etched with an appropriate reagent which preferentially attacks the amorphous fraction of the polymer. SEM examination of such samples revealed two populations of spherulites with quite different contrasts, which were unambiguously associated with the two crystalline structures. The α-spherulites have a dark aspect while the β-ones are very bright. These contrast effects are discussed in terms of the topology of the etched surface. For the α-spherulites, whose lamellae are straight and finely interlocked along the radial and tangential directions, the etched sections are very smooth and consequently the lateral diffusion of normal incident electrons is weak. In contrast, the β-spherulites are characterized by curved lamellae and sheaf-like structures, thus making the surface rougher after etching, and which contribute to the emission of more secondary electrons to the detector. This interpretation is confirmed by the corresponding contrast observed in metallographic microscopy using low-angle illumination.

(Keywords: isotactic polypropylene; scanning electron microscopy; spherulites)

INTRODUCTION

Because of the variety of its crystalline structures, isotactic polypropylene (PP) is one of the most complex of the commercially developed polymeric materials. At least three different crystal cells are commonly encountered. The first of these is the monoclinic α-form which was characterized by Natta *et al.*[1]. The second form, which crystallizes over a particular range of crystallization temperatures and/or under specific rheological conditions, is the hexagonal β-form[2,3]. Thirdly, the γ-form, with a triclinic cell, can be isolated by solvent fractionation from low-molecular-weight PP samples, but the yield of product using this process is very low[3,4]. Consequently, the α- and β-phases dominate in the crystallization of the PP grades used in most industrial applications.

In conjunction with diffraction techniques, the polarizing optical microscope has been widely used in previous studies to investigate the influence of the crystallization conditions on the spherulitic structure in PP films[2,5]. It was thus shown that, in most cases, each spherulite is essentially composed of a single crystalline phase. Furthermore, upon quenching a sample from the melt (at a temperature higher than 175°C) to a temperature above 132°C, only the α-form is produced. With lower crystallization temperatures, the β-form always appears, either in greater or lesser proportions.

Although the γ-form is not particulary important by itself, on account of its minor occurrence, it has been suggested[6] that crystallites of the γ-form could be involved in the growth of the tangent lamellae in the cross-hatched α-spherulites, with the a- and c-axes of the radial lamellae being parallel to the $-a$- and $-c$-axes of the tangential lamellae. A resulting mismatch of 2.3% arises if one considers that there are only monoclinic crystals in the cross-hatched α-spherulites, while the mismatch is reduced to just 0.6% if there is some participation of the γ-phase. However, other workers[5,7] have disputed the role of the γ-form in the tangential growth of these lamellae and attributed the latter solely to an epitaxial effect[8].

Although these investigations have revealed the main features of PP crystallinity, they are based on observations performed almost exclusively on thin films which were obtained either by casting samples between glass plates, or by microtoming the material. Despite the usefulness of these techniques for detailed analysis of the crystalline phases, they are not suitable for structural characterization of bulk samples, for example, the *in situ* characterization of spherulite evolution during the course of tensile testing when using a thick testpiece. For such experiments, the scanning electron microscope is a particularly well suited instrument, especially

*To whom correspondence should be addressed

0032-3861/93/234817-09

since specific etchants[9–12] have been developed which are capable of revealing the spherulite substructure. However, to date, the different crystal modifications could not be identified directly from scanning electron microscopy (SEM) observations. It is the aim of this paper to solve this problem, by analysing the different contrasts of the spherulites in bulk samples which contain both the α- and β-phases.

MATERIAL AND METHODS

Material

The polypropylene used in this work was manufactured and processed by Atochem (3050 MN1). This natural isotactic grade has a relatively broad molecular weight distribution, as assessed by gel permeation chromatography (g.p.c.), with $M_w = 75\,940\ g\ mol^{-1}$ and $M_n = 262\,200\ g\ mol^{-1}$. Pellets of the polymer were subsequently processed by intrusion in a thick mould ($300 \times 200 \times 15$ mm) designed for producing parallelepipedic plates. This technique consists in slowly extruding the melt in the mould and continuing the mould feeding under the extruding pressure during the cooling sequence. The samples thus obtained have negligible orientation, and possess much less chain degradation and contain less bubbles than those formed from conventional injection or extrusion techniques. In addition, the cooling is relatively slow and the semicrystalline structure is quite reproducible. The processing consists of filling the mould (which is maintained at 30°C) with the polymer at a temperature of 230°C, under a pressure of 6 MPa. The cooling time is ~ 240 s.

Sample preparation for SEM observations

PP cubes were cut out of the intruded material such that two of the faces corresponded to the larger surfaces of the original plates. The cutting operation was carried out using a special technique involving a carborundum-impregnated wire, so that no damage was caused to the structure. One lateral face of the cube, chosen for surface-to-surface observation of the structure, was progressively abraded using several different emery papers, and was then finally polished with a very fine alumina powder (0.1 μm) until it was highly flat and smooth, with no visible scratches. The samples were then immersed for 18 h in the solution recommended by Olley *et al.*[9] for the observation of spherulitic structures in PP, i.e. 1.3 wt% potassium permanganate, 32.9 wt% concentrated H_3PO_4 and 65.8 wt% concentrated H_2SO_4. This permanganic acid solution preferentially etches the amorphous part of the polymer in the spherulites, in such a way that the lamellae then appear clearly. Subsequently, the specimens were carefully washed with hydrogen peroxide, distilled water and acetone in order to avoid any artefacts caused by pollution effects. They were finally sputtered with a very thin layer of gold in order to eliminate any undesirable charge effects during the SEM observations. The instrument used in these studies was a standard JEOL SEM 820 microscope. All of the images presented in this paper were obtained using the secondary electron mode, with the primary scanning beam being accelerated under a high voltage ($\leqslant 15$ kV).

Complementary structural techniques

In addition to the samples prepared for the SEM observations, several other specimens were carefully cut out of the intruded PP plates, either near the mid-thickness plane or near the surface, for structural investigations using various other techniques. Some of these specimens were used in transmission X-ray diffraction experiments using a Siemens D500 goniometer, equipped with a $CoK\alpha_1$ monochromator and a digitized linear counter (Inel CPS120). Other samples were examined by differential scanning calorimetry (d.s.c.), using a Setaram 11 instrument operating a heating rate of $5°C\ min^{-1}$. In addition, a number of samples were subjected to densitometric measurements, which involved determinations of the weight differences in air and in pure methanol.

IDENTIFICATION OF THE α- AND β-SPHERULITES

Scanning electron microscopy

The micrographs given in *Figures 1a* and *1b* show typical views of the microstructure, close to the surface, and at the plate core, respectively. From these pictures (presented at the same magnification) one can observe that the spherulitic structures are quite different in the two zones. Near the surface (*Figure 1a*) the spherulites are small, with an average diameter of $\sim 30\ \mu$m, and exhibit a very dark contrast. On the other hand, the spherulites near the mid-thickness plane (*Figure 1b*) have a much larger diameter, which is greater than 100 μm in most cases. Moreover, they clearly separate into two families, with some of them being dark, similar to the surface spherulites, while the others appear with a much brighter intensity. At a higher magnification (see

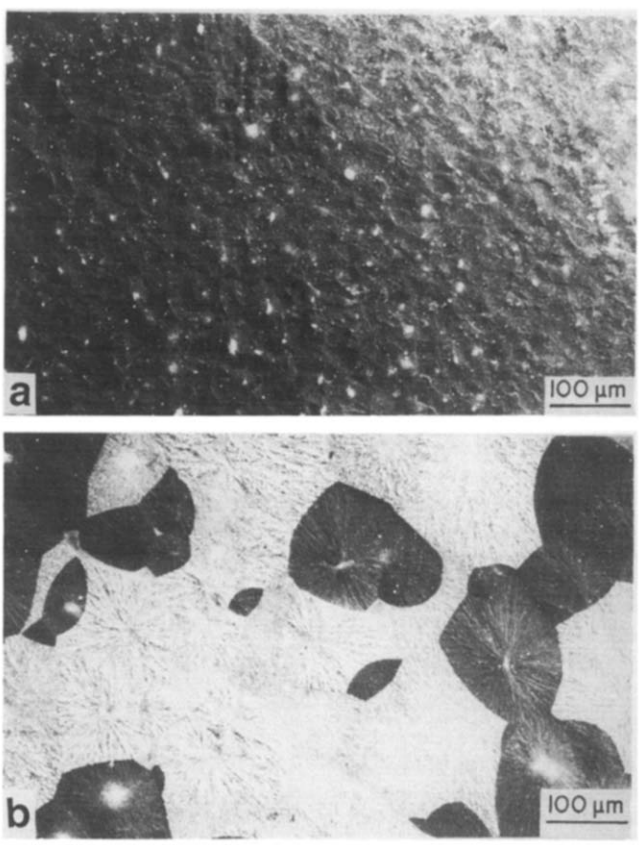

Figure 1 Scanning electron micrographs showing general views of the spherulitic structure in a PP plate: (a) close to the surface and; (b) at the core

Figures 2a and *2b*) the two types of core spherulites are seen to contain different lamellar substructures: the lamellae appear as nearly rectilinear in the dark spherulites, while they seem to be sinuous and probably curved in the bright ones.

In order to study the influence on the structure of the position from the surface, in a more quantitative way, a complete set of micrographs was taken at increasing depths from the surface to the mid-thickness plane, and these are displayed in *Figure 3*. This analysis confirms the preliminary observations made from *Figures 1* and *2* and provides additional information about the surface-to-core transition. It is noted that only dark spherulites are present in the first half-millimetre below the surface, while the first bright spherulites are observed at a depth of ~ 1 mm. From this series of micrographs, it is evident that the relative proportion of the bright spherulites increases progressively with increasing distance from the surface, until they eventually become the major species. Taking account of the equiaxial shape of both kinds of spherulites, the respective proportion (by volume) was deduced as a first approximation from their surface fractions which were measured directly from the micrographs. For each thickness, a reliable value of this proportion was determined by averaging measurements carried out on several micrographs. In this way it was found that the bright spherulites occupy up to 64 vol% of the material in the mid-thickness plane of the intruded samples.

X-ray diffraction

The X-ray diffraction patterns of surface and core specimens of a PP plate are displayed in *Figures 4a* and *4b*, respectively. In both cases it can be seen that there is a rather broad hump at $2\theta \approx 20°$, which is characteristic of the amorphous component. Sharp peaks are superimposed on the latter, due to diffraction by the crystalline lamellae. In the surface material (*Figure 4a*), analysis of these diffraction peaks reveals that the crystalline fraction is composed entirely of the monoclinic α-form. In contrast, the core samples produce a more complex diffraction pattern (*Figure 4b*). In addition to the peaks representing the α-form, a completely new set of peaks appear, which are characteristic of the hexagonal β-form. In particular, the highest peak, located between the 110 and the 040 reflections of the α-crystals, corresponds to the 300 reflection of the β-phase. Otherwise, indexing of the X-ray pattern reveals no significant traces of the γ-form.

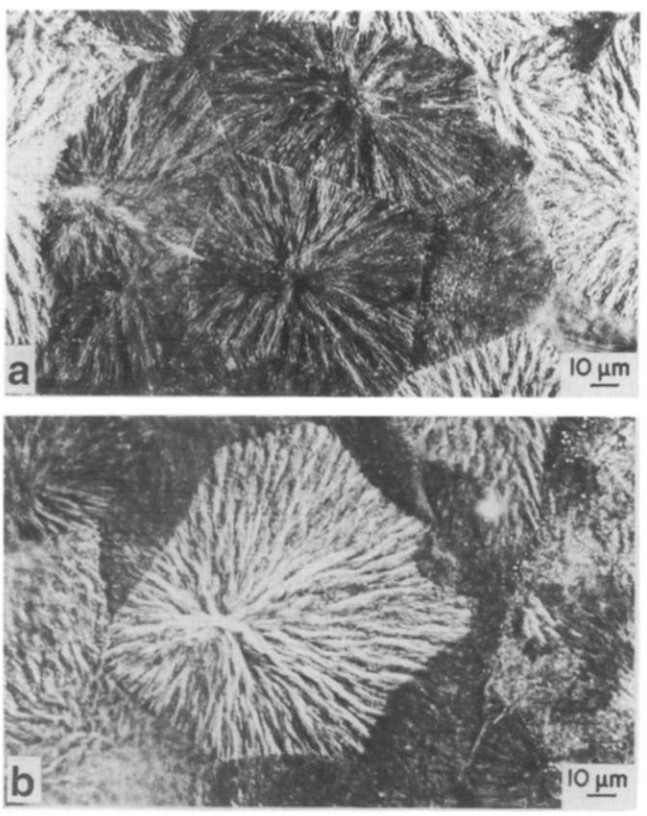

Figure 2 Scanning electron micrographs of the same views of the spherulitic structure of PP as shown in *Figure 1*, but shown at a higher magnification: (a) close to the surface and; (b) at the core

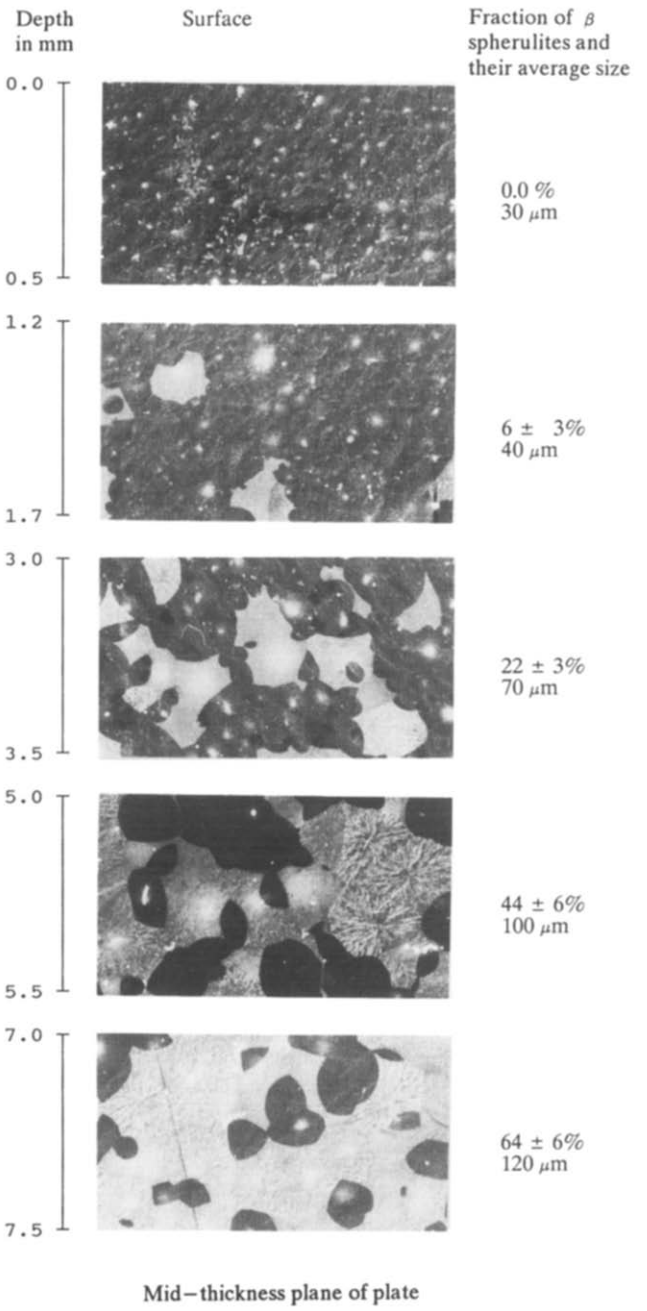

Figure 3 Scanning electron micrographs taken at regular intervals in depth from the surface to the core of a PP plate

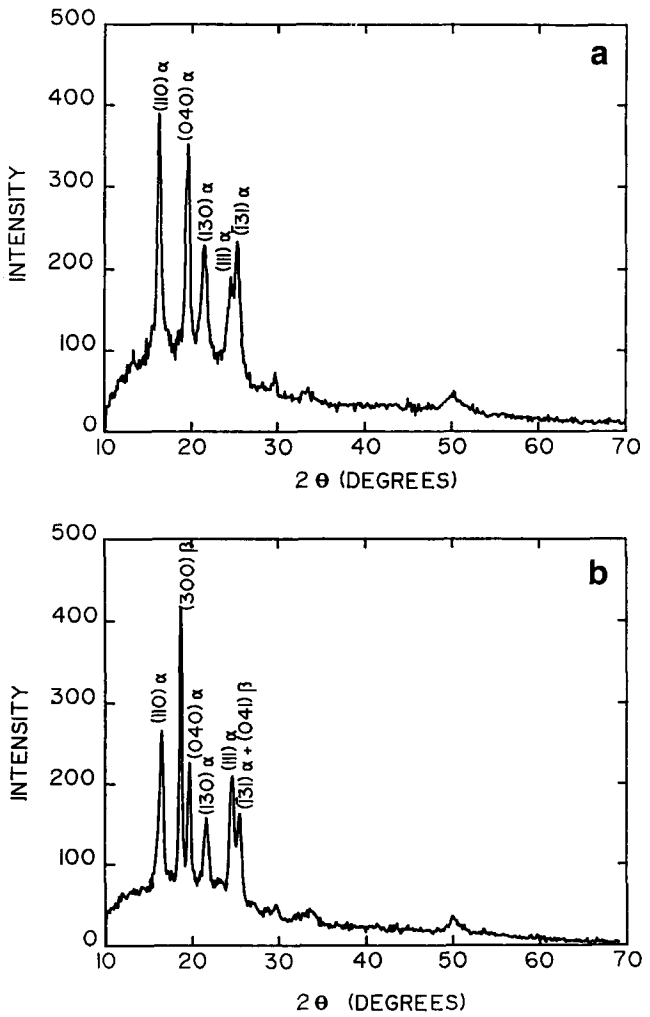

Figure 4 X-ray diffraction patterns of a PP plate obtained for samples taken: (a) from the surface region and; (b) from the core region

The proportions of the α- and β-forms in the crystalline part of the core specimen were evaluated from the above diffraction patterns by using the method of Turner-Jones *et al.*[3]. These authors only take into account the 110, 040 and 130 peaks of the α-form, and the 300 peak of the β-form. The proportion of the β-phase is therefore given by the following relationship:

$$f_\beta = h_\beta(300)/[h_\alpha(110) + h_\alpha(040) + h_\alpha(130) + h_\beta(300)] \quad (1)$$

where $h_i(hkl)$ represents the height of the hkl peak of the i-form above the amorphous hump. In principle, the proportions obtained by this method refer to the relative mass of each phase. However, since the densities of the two crystal cells are very close ($\rho_\alpha = 0.945\ g\ cm^{-3}$ cf. $\rho_\beta = 0.921\ g\ cm^{-3}$), we can consider that f_β also represents the volume proportion of the β-phase. The values obtained by this method are given in *Table 1*, which also shows the index of crystallinity for each specimen, obtained from the area under the crystalline peaks divided by the total area under the diffraction curve, following the method of Hermans and Weidinger[13,14].

Differential scanning calorimetry

The d.s.c. thermograms displayed in *Figures 5a* and *5b* were obtained from specimens cut from the surface and core regions, respectively. The curve shown for the surface material displays a single endotherm at ~170°C, which is clearly related to the α-phase[6], and is thus confirmed to be the only phase present in these surface specimens. In contrast, in the thermogram obtained for the core sample, one can see two different peaks, at 155 and 170°C, which represent melting of the β- and α-forms, respectively, in agreement with the X-ray diffraction results.

These fusion thermograms offer an alternative way of quantitatively assessing the proportions of the crystalline phases. If one assumes that the enthalpy of fusion is similar for both crystalline forms ($\Delta H_{f_c} \approx 165\ J\ g^{-1}$, after Wunderlich[15]) the index of crystallinity (volume fraction) can be written as:

$$X_c = \frac{\rho \Delta H_f}{\rho_c \Delta H_{f_c}} \quad (2)$$

Table 1 Index of crystallinity and relative proportion of β-phase in surface and core specimens of PP, deduced from the X-ray diffraction profiles

Specimen	X_c (%)	f_β (%)
Surface	40±5	0
Core	52±5	50±9

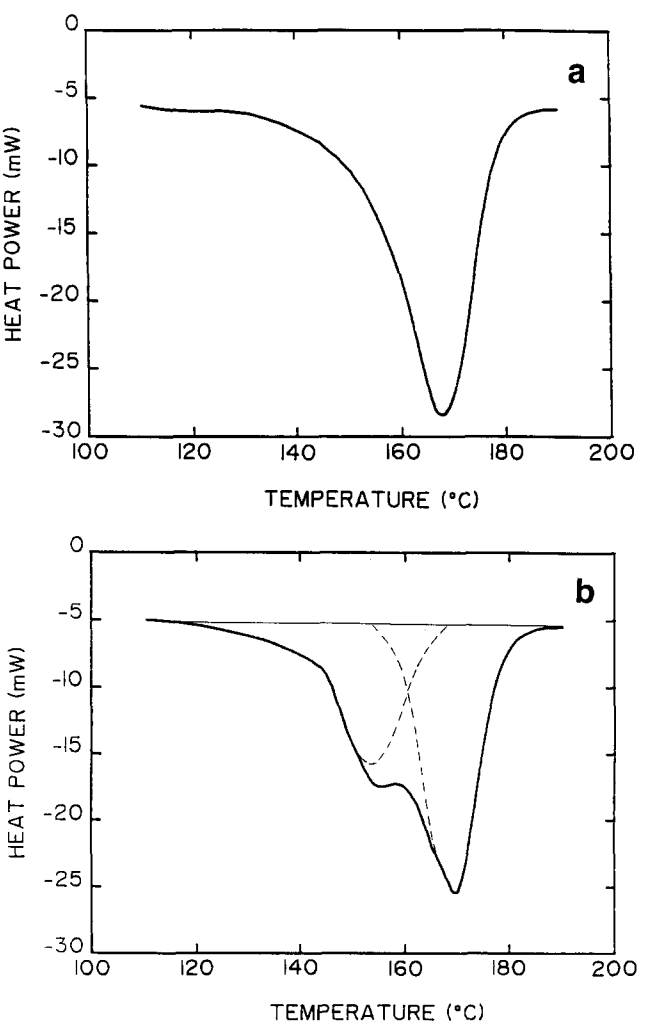

Figure 5 D.s.c. thermograms of a PP plate obtained for samples taken: (a) from the surface region and; (b) from the core region

where ΔH_f is the total enthalpy of fusion of the specimen, ρ is its density and ρ_c is the crystalline density (assumed to be equal for both forms, as above). Using the same assumptions, the relative proportion of the β-phase can also be obtained by using the relationship:

$$f_\beta = \Delta H_\beta / \Delta H_f$$

The d.s.c. results are displayed in *Table 2*.

These results confirm those previously obtained by the X-ray diffraction measurements, even if there is a slight difference in the X_c and f_β values; this is probably due to the approximations made in both approaches.

Density measurements

The densities of samples which have been taken from the surface and from the core of the PP specimens are shown in *Table 3*. It is noted that the core material is slightly denser than the surface material. Following a classical derivation[16], this difference in density is correlated to the difference in the volume index of crystallinity by means of the following relationship:

$$X_c = \frac{\rho - \rho_a}{\rho_c - \rho_a} \quad (3)$$

where ρ is the measured density of the specimen, $\rho_c = 0.933\ g\ cm^{-3}$ (the average density of the two crystalline modifications) and $\rho_a = 0.854\ g\ cm^{-3}$ (the amorphous density, deduced by extrapolation from the molten state)[15]. These calculated values of X_c are also reported in *Table 3*.

The data obtained in this way again show that the core material is somewhat more crystalline than the surface layers, due a the faster cooling rate for sample in contact with the mould, when compared to that of the bulk material.

Discussion of the crystallization kinetics of the two PP phases

All of the results obtained above from analytical methods and microscopic observations appear to suggest that the dark spherulites are crystallized in the α-form and the bright spherulites consist of β-crystallites. We will now examine the interrelation of the structure with its depth from the surface of the sample.

The samples that we analysed were taken from plates which were obtained by the intrusion process. The cooling rate for the material was therefore highly inhomogeneous, as the surface of the plate was quenched while the bulk of the sample took a very long time to cool. As observed above, there are only α-spherulites close to the surface, while the β-phase represents 50–65% of the crystalline content near the mid-thickness plane. It is also interesting to note that in the dual-phase region: (i) the β-spherulites have a larger size than the α-spherulites, even if the β-phase occupies, on the whole, a smaller volume fraction and; (ii) the inter-spherulitic boundary between the α- and β-types is always curved, with the concavity oriented towards the α-phase. One could speculate from these facts that germination of the β-spherulites begins earlier than that of the α-spherulites. Obviously, this is not true since the melting point of the α-phase is some 15°C higher than that of the β-phase. It is more likely that the crystallization rate of the β-phase is faster than that of the α-form. This behaviour was actually verified by Padden and Keith[2], who found a difference of approximately 20% between the two crystallization rates over the temperature range from 110 to 140°C. One can readily imagine that the faster growth rate of the β-spherulites is correlated, to some extent, to their simpler lamellar morphology, in contrast to the complex cross-hatched crystallites in the α-spherulites[17,18]. We will discuss below why there are only α-spherulites close to the surface and also why a dual-phase structure exists in the core.

The surface regions of the plates are typically subjected to a non-isothermal crystallization with a very high cooling rate. Under such conditions, Varga has shown in a recent paper[19] that the β-phase has very little chance to be nucleated and, even if some β-spherulites did appear during the initial stages of cooling, they would rapidly change their growing lamellae into the α-structure as soon as the critical temperature, $T_{\alpha\beta}$ (≈ 100°C), is reached[20,21]. This is the reason why no measurable amounts of the β-phase were revealed by X-ray diffraction nor by d.s.c. measurements on the surface specimens.

In contrast, the cooling rate in the core is very slow, and the proportion of the final phase is controlled by the growth rate, which is more favourable for the β-spherulites. According to earlier work[22], another factor influencing the growth rate is the internal stress that is developed in the core of the plate during the intrusion process. This is due to a hindrance to contraction which is imposed on the core material by the surface layers which solidify rapidly while the centre of the plate is still liquid. This effect also favours the development of the β-phase.

Table 2 Index of crystallinity and relative proportions of β-phase in the surface and core specimens of PP, deduced from d.s.c. measurements

Specimen	ΔH_β ($J\ g^{-1}$)	ΔH_f ($J\ g^{-1}$)	X_c (%)	f_β (%)
Surface	0	81±5	47±4	0
Core	45±5	87±5	51±4	52±8

Table 3 Index of crystallinity of the surface and core specimens of PP, deduced from density measurements

Specimen	ρ ($g\ cm^{-3}$)	X_c (%)
Surface	0.898±0.001	55±1
Core	0.900±0.0015	58±1

ORIGIN OF THE CONTRAST DIFFERENCE BETWEEN THE α- AND β-SPHERULITES

Comparison between electronic and metallographic micrographs

One of the PP samples was subjected to comparative observations by using the scanning electron microscope (*Figure 6a*), and an optical microscope in reflection (metallographic microscopy), under both direct illumination (*Figure 6b*) and low-angle lighting (*Figure 6c*). The shapes of the same spherulites are readily identified in the three views. However, it appears that the types of contrast of the two species do not match in each case: the spherulites which are dark in the scanning electron micrograph (i.e. the α-phase) exhibit a bright contrast under direct light but change to a dark contrast under low-angle

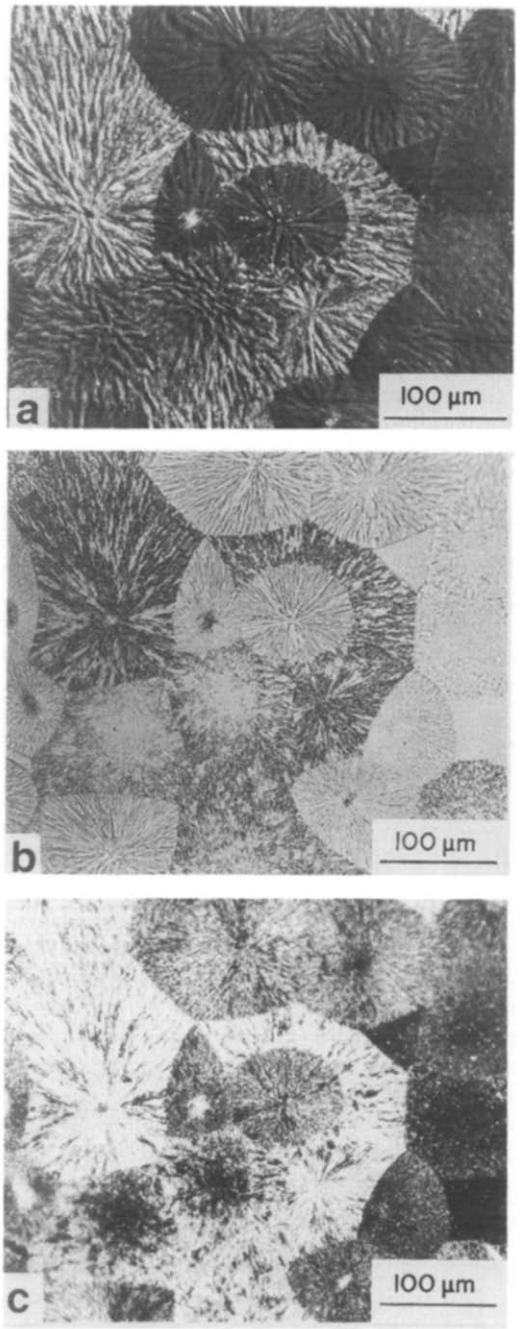

Figure 6 Corresponding observations of the spherulites in a PP plate by using: (a) scanning electron microscopy; (b) metallographic microscopy under direct illumination and; (c) metallographic microscopy under low-angle illumination

illumination. A reciprocal behaviour is observed for the β-spherulites.

Complementary contrast tests were carried out in the SEM studies by taking pictures with different tilt angles of the specimen surface (*Figure 7*). For the inclined positions, it was necessary to correct the defocalization effect resulting from the tilt, particularly at angles greater than 40°. The electron micrographs presented in *Figure 7* show the same region of a sample, which is inclined at tilt angles of 0, 20, 40 and 60°. While no major changes appear between 0° (*Figure 7a*) and 20° (*Figure 7b*), it can be seen that the contrast between the two types of spherulite is enhanced at an angle of 40° (*Figure 7c*), and then dramatically vanishes at 60° (*Figure 7d*). It would have been interesting to see the effect of tilting the sample still further (i.e. towards 90°), but unfortunately the detector geometry of our SEM equipment did not permit this manipulation to be safely achieved. However, it is reasonable to predict that the contrast between the α- and β-spherulites would be eventually inverted at very large tilt angles.

From the above observations that the contrast of the two kinds of spherulites can be modified at will by simply changing the direction of illumination (for optical micrographs) or the inclination of the surface (for electron micrographs), it can be deduced that the origin of the contrast is the same, namely the roughness of the etched surfaces. It is now interesting to examine why the etchant, i.e. permanganic acid solution, develops different surface topologies for the two crystalline phases.

Discussion of the contrast effects

The various spherulite morphologies of isotactic polypropylene were analysed in detail by Norton and Keller[5]. Two types of spherulitic microstructures are encountered in the α-form. Type I spherulites, which appear at a temperature lower than 134°C, exhibit an overall positive birefringence when examined in a polarizing microscope, and they are characterized by cross-hatched lamellae. While the main lamellae are oriented radially, tangential lamellae appear to grow by epitaxial deposition, with a direction of growth which is inclined by approximately 81°[7]. These tangential lamellae are responsible for the sign of the birefringence that is observed. On the other hand, at a crystallization temperature higher than 138°C, negatively birefringent spherulites are also identified. These Type II spherulites are therefore presumed to contain only a small proportion of tangential lamellae, although the amount of transverse lamellae that is necessary to change the birefringence sign cannot be estimated easily. Finally, it should be noted that, in addition to the 'pure' types of spherulite (i.e. I and II), one also finds a large amount of mixed spherulitic species. These are a consequence of the inhomogeneity of the spherulites, where regions of predominantly radial lamellae, giving a negative birefringence, coexist with other regions which contain predominently tangential lamellae which give a positive birefringence[5].

The spherulites of the β-form consist of radially growing lamellae, as in most other semicrystalline polymers. For this structure, two types of spherulite have also been identified. In the case of Type III spherulites, which are produced at a crystallization temperature below 122°C, the lamellae grow rigidly and the microscopic contrast is uniform under polarized light. In contrast, in the Type IV spherulites, the direction of the optical axes changes along the spherulite radius, as a result of the periodic occurrence of lamellae in both a 'face-on' and an 'edge-on' arrangement. Because of this lamellar twist, the spherulites exhibit a 'banded' aspect. This latter form appears over the temperature range from 126 to 132°C.

In the bulk samples investigated in this work, the β-phase dominates in the middle plane of the plate (at a level of approximately 65 vol%), which indicates that the crystallization temperature in this zone was lower than 132°C and that the α-phase consists of either Type I or Type II spherulites (plus some mixed structure as well). Furthermore, crystallization

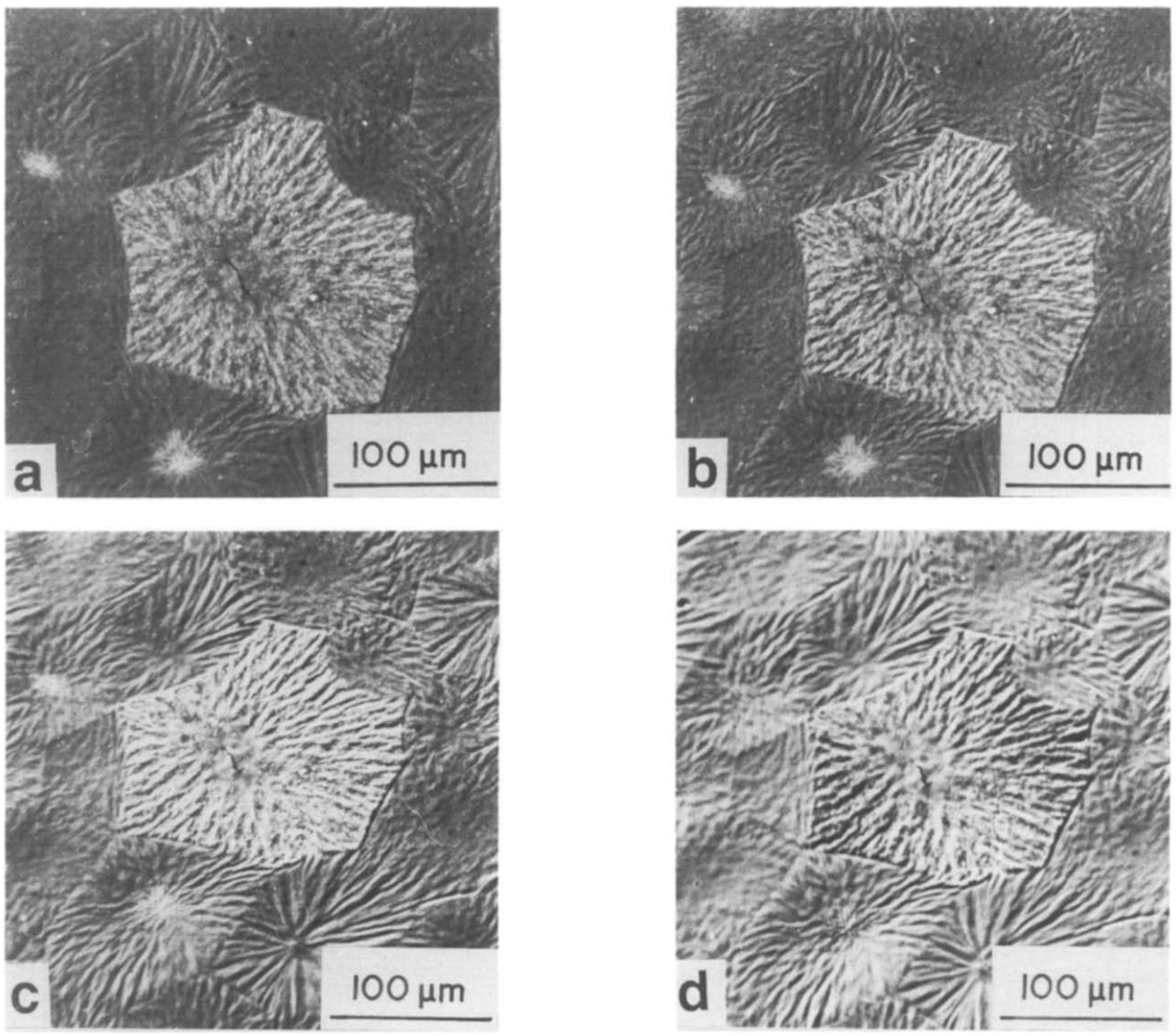

Figure 7 Effect of tilting the sample in SEM observations of a PP plate, shown for tilt angles of: (a) 0°; (b) 20°; (c) 40° and; (d) 60°

took place during continuous cooling of the plate, so that the density of tangential lamellae probably increased as the crystallization temperature decreased[2]. Consequently, although the resolution of the scanning electron microscope is not high enough to observe the individual crystallites, it is highly probable that the α-spherulites are composed of finely interlocked lamellae with both radial and tangential orientations.

As with the β-spherulites, many of the micrographs (see *Figures 2b* and *6b*) clearly show a sheaf-like structure when a spherulite is cut at its middle plane. Most of these spherulites are made of curved lamellae and thus correspond to the Type IV form previously identified in the literature. However, in the micrograph of *Figure 6a*, the bright spherulite containing straight lamellae more closely corresponds to the Type III microstructure, consistent with the fact that it is smaller than the average Type IV spherulites.

In previous studies, Padden and Keith[2] found, for thin films observed in the polarizing microscope, that the β-spherulites could also be identified by their very bright contrast. However, what we see here in the electron microscope has obviously nothing in common with these observations, since the origin of the contrast is of a topological nature. All of our micrographs were obtained by using secondary electrons, and, except for the special series of micrographs shown in *Figure 7*, the sample was always positioned in such a way that its surface was perpendicular to the electron beam. Therefore, the difference in the contrast between the two phases can be explained in the following way.

In scanning electron microscopy, the brightness of the image is related to the number of electrons that are scattered from the sample surface towards the detector. For an ideally flat surface, it has been shown[23] that the secondary electron coefficient (i.e. the yield of secondary electrons) is given by $\delta = \delta_0 \sec \theta_s$, where θ_s is the specimen tilt angle. If the surface is normal to the incident beam (see *Figure 8a*), most of the secondary electrons that are produced are scattered within the sample, with only a few of them being directed out of the sample to the detector. The brightness is therefore very low. In contrast, at a small incidence angle (see *Figure 8b*), the number of secondary electrons that are scattered away from the surface increases and the brightness of the image is therefore much higher.

If the etched PP surfaces are now considered, it is clear that the relief of the surface is much more pronounced

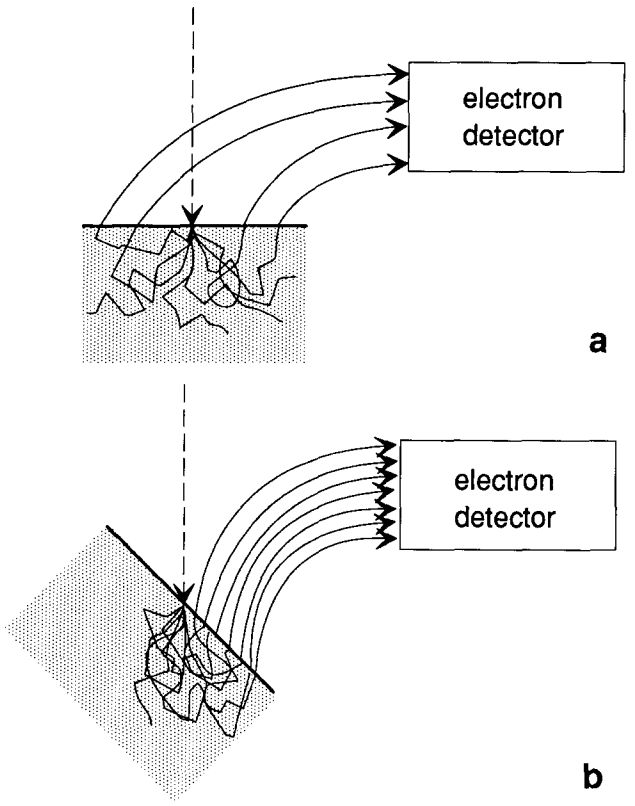

Figure 8 Schematic representation of the tilting effect on the number of secondary electrons emitted toward the detector: the number received by the detector increases with the tilt angle

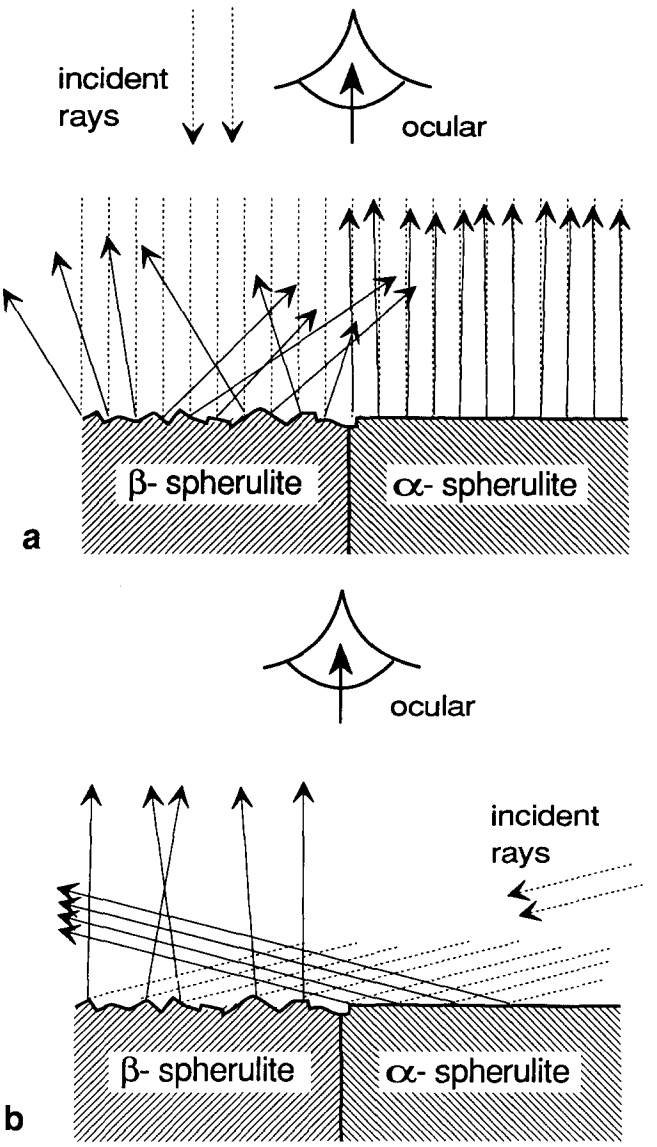

Figure 9 Schematic representation of the reflection of light rays by the etched sections of α- and β-spherulites under conditions of (a) direct and (b) low-angle illumination

at the β-spherulites than at the α-spherulites. This is because the twisted β-phase lamellae are preferentially revealed by the acid etching, while the interlocked network of parallel α-lamellae are more resistant to attack by the etchant. Consequently, for a sample in normal orientation (as in *Figure 7a*), the 'wavy' surfaces of the β-lamellae will release more secondary electrons to the detector and the corresponding spherulites will appear brighter than the α-species. When the tilt angle is increased (see *Figure 7b*) the contrast of the β-spherulites is further increased due to the overall inclination of the surface, while the very smooth α-spherulites still hardly appear. For a tilt angle of 40° (see *Figure 7c*) the latter now begin to emerge and eventually, when the sample is tilted by an angle of 60°, the number of electrons that are emitted by both of the spherulitic structures becomes comparable and their contrast disappears (see *Figure 7d*). This last micrograph has been produced by varying the focal distance along the *z*-axis in order to enlarge the image along the *y*-axis. However, this correction does not have any effect on the evolution of the contrast.

The above interpretation is confirmed by the complementary metallographic micrographs, which show the β-spherulites having a dark aspect under direct illumination (see *Figure 6b*). In this case, most of the incident light rays are scattered by the rough surface and do not reach the ocular (see *Figure 9a*). Conversely, the bright aspect of the α-spherulites is due to the normal reflection of the incident beam by the very smooth surface. The above arguments still hold for observations made under low-angle illumination. In this case, the inversion of the spherulite contrast is simply due to the orthogonality of the incident illumination to the ocular direction (see *Figure 9b*).

CONCLUSIONS

The complex spherulitic structures of polypropylene samples were investigated by scanning electron microscopy after a suitable chemical etching treatment. Two kinds of spherulites were differentiated by their contrast, with some dark and the others bright. Using different analytical methods (d.s.c., X-ray and densitometry) it was proved, quantitatively, that the dark spherulites crystallized in the monoclinic α-form, while the bright ones consisted of the hexagonal β-type. The difference in the observed contrasts is interpreted in terms of the lamellar structure of the individual phases. Because of the preferential etching of the β-spherulites by the permanganic reagent, their surfaces exhibit a much rougher profile than the α-spherulites, which is not dependent on where the spherulites are cut from the sample. This is due to the different crystallite morphologies of the two phases, with the β-lamellae being irregularly twisted, while the α-phase is presumably interlocked in a cross-hatched array of radial and tangential lamellae. Therefore, when the specimens are oriented perpendicular to the direction of the electron

beam, the β-surfaces scatter the secondary electrons more efficiently than the α-sections, and thus more secondary electrons reach the detector in the former case. Consequently, it appears that the structure of bulk samples of polypropylene can be readily investigated by a simple SEM examination, at a much higher resolution than when using the polarizing microscope.

ACKNOWLEDGEMENT

The authors are indebted to Dr Bruno Echalier, of Atochem (Cerdato, Serquigny, France) for kindly providing the polypropylene plates.

REFERENCES

1 Natta, G., Gorradini, P. and Cesari, M. *Rend. Acad. Naz. Lincei.* 1956, **21**, 365
2 Padden, F. J. and Keith, H. D. *J. Appl. Phys.* 1959, **30**, 1479
3 Turner-Jones, A., Aizelwood, J. M. and Beckett, D. R. *Makromol. Chem.* 1964, **75**, 134
4 Addink, E. J. and Beintema, J. *Polymer* 1961, **2**, 185
5 Norton, D. R. and Keller, A. *Polymer* 1985, **26**, 704
6 Padden, F. J. and Keith, H. D. *J. Appl. Phys.* 1973, **44**, 1217
7 Khoury, F. *J. Res. Natl. Bur. Stand.* 1966, **A70**, 29
8 Clark, E. S. and Spruiell, J. E. *Polym. Eng. Sci.* 1976, **16**, 176
9 Olley, R. H., Hodge, A. M. and Basset, D. C. *J. Polym. Sci., Polym. Phys. Edn* 1979, **17**, 627
10 Olley, R. H. and Basset, D. C. *Polymer* 1982, **23**, 1707
11 Basset, D. C. and Olley, R. H. *Polymer* 1984, **25**, 935
12 Olley, R. H. and Basset, D. C. *Polymer* 1989, **30**, 399
13 Hermans, P. H. and Weidinger, A. *Makromol. Chem.* 1961, **44–46**, 24
14 Hermans P. H. and Weidinger, A. *Makromol. Chem.* 1961, **50**, 98
15 Wunderlich, B. 'Macromolecular Physics', Academic, New York, 1973
16 Schultz, J. 'Polymer Materials Science', Prentice-Hall, Englewood Cliffs, NJ, 1974
17 Samuels, R. J. and Yee, R. Y. *J. Polym. Sci., A-2* 1972, **10**, 385
18 Jacoby, P., Bersted, B. H., Kissel, W. J. and Smith, C. E. *J. Polym. Sci., Polym. Phys. Edn* 1986, **24**, 461
19 Varga, J. *J. Mater. Sci.* 1992, **27**, 2557
20 Lotz, B., Fillon, B., Thierry, A. and Wittmann, J. C. *Polym. Bull.* 1991, **25**, 101
21 Varga, J. and Toth, F. *Makrom. Chem., Makromol. Symp.* 1986, **5**, 213
22 Duffo, P. *PhD Thesis* Ecole des Mines de Paris, France, 1990
23 Goodhew, P. J. and Humphreys, F. J. 'Electron Microscopy and Analysis', Taylor and Francis, London, 1988